

Improving the mechanical properties of CNF films by NMMO partial dissolution with hot calender activation

Hannes Orelma · Antti Korpela · Vesa Kunnari · Ali Harlin · Anna Suurnäkki

Received: 24 November 2016 / Accepted: 16 February 2017 / Published online: 24 February 2017
© Springer Science+Business Media Dordrecht 2017

Abstract Reinforcing of cellulose nanofibril (CNF) films by partial dissolution with *N*-methylmorpholine-*N*-oxide (NMMO) was investigated. The method investigated is composed of impregnation of CNF film with liquid solution of NMMO followed by dry heat activation. The heat activation of the impregnated film was carried out using a heated calendering nip, which enabled simultaneous heating and compression. The partial dissolution of cellulose by NMMO caused a significant increase in the transparency of CNF film due to the decrease of film porosity and increased surface smoothness. The dry strength of the reinforced film was increased from 122 up to 195 MPa. Furthermore, the wet strength of the reinforced film was up to 70% greater than the dry strength of pure CNF film. The changes in the fibrillar structure were investigated with topographical imaging (SEM and AFM) and spectroscopically using NMR and FTIR. No significant changes in the fibril structure or cellulose morphology were observed. Moreover, the treated film resisted significant water pressure, highlighting

CNF film's permanent water resistance. The partial dissolution process with NMMO was also capable of reinforcing a CNF composite film with macro scale structural elements (lyocell short-cut fibres). The strategy investigated is a robust and fast method to improve the mechanical properties of fibrillary cellulose films, allowing them utilization in applications where improved water resistance and fully cellulosic character are required properties.

Keywords CNF · Film · NMMO · Partial dissolution · Hot calendering

Abbreviations

CNF Cellulose nanofibrils
NMMO *N*-methylmorpholine-*N*-oxidide

Introduction

Cellulose, the most abundant material on earth, (Klemm et al. 2005) has currently obtained higher industrial and scientific visibility due to the drastic demand to compensate for the use of limited, renewable and biodegradable synthetic materials. Wood-based cellulose is the largest cellulose source on earth, and it has already widely been utilized in paper and board applications for decades. Recently, cellulose nanofibres (CNF), (Klemm et al. 2011; Moon et al. 2011) have attracted attention due to their unique

Electronic supplementary material The online version of this article (doi:10.1007/s10570-017-1229-6) contains supplementary material, which is available to authorized users.

H. Orelma (✉) · A. Korpela · V. Kunnari ·
A. Harlin · A. Suurnäkki
High Performance Fibre Products, VTT Technical
Research Centre of Finland, Biologinkuja 7, 02044 Espoo,
Finland
e-mail: hannes.orelma@vtt.fi

properties broadening application potential into areas where macrofibre-containing cellulosic materials are not optimal. CNF has already been utilized in many applications e.g. filaments (Walther et al. 2011; Iwamoto et al. 2011), aerogels (Paakko et al. 2008), rheology modifiers (Hubbe and Rojas 2008), and films (Syverud and Stenius 2009; Österberg et al. 2013). Many studies have shown that films made from CNF have an excellent strength to weight ratio, and also some special features such as a good oxygen barrier property (Henriksson et al. 2008; Lavoine et al. 2012). However, the application potential of CNF films has been limited because of their inherent insufficient waterproofness, which limits the utilization of these films in applications where they should be in contact with the aqueous environment. Waterproofness of the CNF film can be improved with hydrofobizing agents, wet strength agents, and by chemical cross-linking treatments (Qing et al. 2013; Spoljaric et al. 2013; Kurihara and Isogai 2014; Toivonen et al. 2015). However, those modification routes have not yet shown their feasibility in practice. Potential products made from wet strength CNF (WS-CNF) films could be found around packaging films such as wrapping and protective films, and light-weight shopping and rubbish bags. In agriculture and horticulture, WS-CNF-films film could possibly be used as a biodegradable, environmentally friendly option for mulch films, low tunnel film or even as greenhouse films, all made predominantly from polyethylene (Briassoulis 2004; Kapanen et al. 2008).

A relatively new approach to improve the mechanical performance of cellulosic materials is the all-cellulose concept with partial dissolution, or adding dissolved cellulose materials into cellulosic matrixes (Huber et al. 2011). This fusion does not change the chemical properties of cellulose and the material retains its inherent hydrophilicity. The partial dissolution and impregnation using pre-dissolved materials utilizes the ability of some chemicals to interrupt the hydrogen bonding of cellulose via direct or derivatizing dissolution, making the treated cellulose material soluble into a utilized medium (Klemm 1998). Partial dissolution of a fibrous material means the partial solubilization of the outer surfaces of cellulose material subunits, which subsequently can be embed via inter-fibril entanglement and crystallization when the solubilized material is regenerated, causing “solvent welding” for the material structure. The most

used solubilizing agents used with cellulosic materials are *N*-methylmorpholine-*N*-oxide (NMMO) (Johnson 1969), LiCl/DMAc (Nishino and Arimoto 2007), NaOH/Urea (Vanderhart and Atalla 1984), and ionic liquids (Graenacher 1934), which have already shown their application potential with fibrous cellulosic materials. In the present study, low toxic NMMO, the industrially used non-derivatizing cellulose solvent, was used on the partial dissolution of cellulose nanofibrils (CNF) films for improving the film mechanical performance.

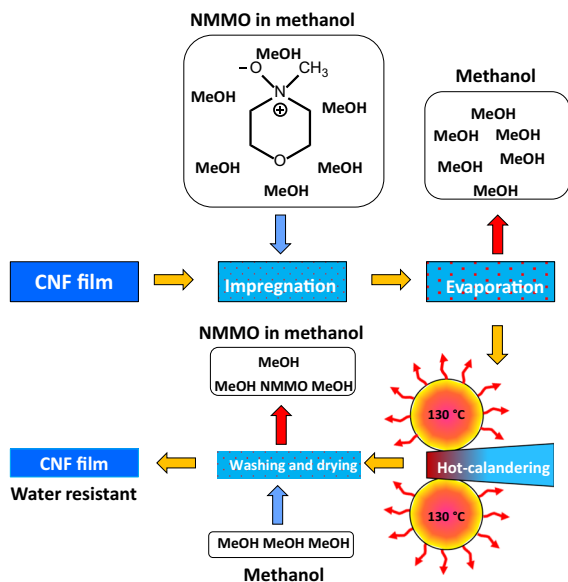
N-methylmorpholine-*N*-oxide (NMMO), in aqueous solutions, has the ability to dissolve cellulose in high concentrations without alteration of the chemical structure of the cellulose (Fink et al. 2001). The dissolution mechanism is under dispute, but it is speculated that the ability arises from the highly polar N–O dipoles of a NMMO molecule, which can form bonds with the cellulose resulting in disruption of the crystalline structure of the cellulose (Rosenau et al. 2001; Fink et al. 2001). However, the complete dissolution of cellulose using NMMO is highly dependent on the processing conditions, and typically the optimal conditions are: water content between 10 and 13% and temperature above 100 °C (Wachsmann and Diamantoglou 1997; Chanzy et al. 1982). Furthermore, one advantage of NMMO is its substantially easy chemicals recycling pathway due to the monocomponent system.

The aim of the study was to investigate a method to improve the mechanical and water resistance performance of pre-made CNF films by using the all-cellulose concept with the partial dissolution strategy with NMMO. The second task of the study was to investigate a suitable methodology to control the dissolution process. The process used in this study is presented schematically in Scheme 1. The investigated reinforcement route allows producing water-resistant CNF-films without adding extra materials to a CNF film.

Experimental

Materials

Cellulose nanofibrils (CNF) were obtained by processing bleached sulphite pine pulp (Consistency 1.5%) through a Masuko grinder with three passes with subsequent fluidization (at least six passes) by a M110P microfluidizer (Microfluidics corp., Newton,



Scheme 1 Schematic illustration on the partial dissolution of cellulose nanofibrils (CNF) film with NMMO by utilizing the heat activation by a hot calender

MA, USA). The microfluidizer was equipped with a chamber pair (400 and 100 μm chambers) and operated at 2000 bar pressure. The CNF used in the Surface Plasmon Resonance (SPR)-studies was prepared from bleached sulphite birch pulp similar to that described above. 4-Methylmorpholine-*N*-Oxide monohydrate (NMMO, # 67873) was ordered from Sigma Aldrich (Finland). 1.5 denier lyocell short-cut fibres with a 5 mm length were obtained from Engineered fibres technology LCC, Shelton, USA. All other chemicals used in this study were analytical grade.

Methods

Manufacture of cellulose nanofibril (CNF) films

The nanofibril cellulose films used in this study were prepared using the SUTCO CNF film manufacturing environment located at VTT, Espoo, Finland (Persin et al. 2012; Tammelin et al. 2013). In the method, approximately 1.5 wt% CNF (carrying 0.45% of sorbitol or carrying 30% of sorbitol from the amount of dry fibre) was solvent cast on a polypropylene film. On drying, the CNF adheres to the polypropylene film, which prevents film shrinkage. The sorbitol was utilized as a plasticizer to soften otherwise brittle

CNF films. The wet CNF web was allowed to dry overnight, followed by manual delamination from the PP-film. The prepared continuous CNF film was cut into A4 size sheets and stored in 50% RH, 23 °C. The dry thickness of the prepared films was $27.6 \pm 0.4 \mu\text{m}$ and density $1430 \pm 50 \text{ kg/m}^3$.

The CNF films carrying 5 mm long 1.5 denier lyocell short-cut fibres were prepared by first mixing dry short-cut fibres into CNF gel with a DAC 1100 high speed mixer (IGT Testing Systems Pte. Ltd., Singapore). The short-cut fibre consistency in the prepared films was 5% of the dry weight of CNF. The CNF-short-cut fibre solution was manually spread on a polypropylene film and allowed to dry overnight in the standard lab conditions (50% RH, 23 °C). The prepared CNF composite films dry thicknesses were $43.4 \pm 0.9 \mu\text{m}$ and density $894 \pm 69 \text{ kg/m}^3$. The prepared films were stored under 50% RH.

Improving the mechanical properties of CNF films by partial dissolution with NMMO

The reinforcement of the CNF films was carried out by using a partial dissolution strategy with NMMO (Johnson 1969). NMMO was dissolved into methanol–water solution with varying water content (from 0 to 50 wt%). The NMMO consistency of the solution varied between 10 and 35 wt%. After complete dissolution of NMMO, a pure CNF film without any pre-treatment was placed in the NMMO solution for 2 h. Then the impregnated films were drained briefly and subsequently dried between blotting boards overnight before heat activation with a heated calender nip. The NMMO solution did not contain a stabilization agent as propylgallate, which is typically used in dissolution processes of cellulose to prevent unwanted side reactions and cellulose chain degradation due to the dry processing condition and low chemical amount in the impregnated CNF film.

The heat activation of the dry NMMO-impregnated CNF film was carried out with a self-made calender. The calender comprised of a lower rubber-coated roll and an upper heated smooth steel roll equipped with the surface temperature control (Figure S1, supporting information). The impregnated film was passed through the calender nip twice by using a constant temperature of 130 °C, speed of 1 m/min, and line load approximately 20 kN/m. With the selected line load, the nip length was measured to

be 15 mm. The surface temperature of the film was monitored with a portable infrared thermometer so as to assure that the film temperature was raised to 130 °C. After a second pass, the film was released from the metal roll with a sharp blade. After the heat activation, the reinforced CNF film carrying the NMMO was placed in pure methanol for 1 + 1 h to remove the residual NMMO. Finally, the reinforced film was dried between blotting papers until it reached the equalib. The reinforced CNF film was stored in the 50% RH.

Mechanical strength of the reinforced CNF film

The mechanical properties of the prepared CNF films were characterized with a LS5 Lloyd (Ametek Sensors, Test and Calibration, Germany) equipped with a 100 N load cell. The specimens were cut into 15 mm width pieces with a lab paper cutter. The mechanical load was recorded at a constant 0.5 mm/min velocity and grip distance of 40 mm. For calculating tensile strength, the thickness of each specimen was separately measured from each sample prior to tensile testing. The thicknesses were measured from three different places as per a sample using a Lorenzen and Wettre electric micrometre gauge. The tensile strength was calculated using the average thickness of these three measurements. Prior to the measurement, the samples were conditioned in the standard condition at 23 °C and 50% RH for at least 2 days. Prior to the wet measurements, the samples were immersed in water for 24 h and measured when wet. In the wet strength measurements, only the extensional force is shown because of the difficulties of measuring the thickness of swollen films. For both dry and wet strengths, at least seven parallel samples were measured.

Liquid up-take of CNF films

The liquid up-take of pure CNF film was carried out with pure methanol with varying water content (the tested water contents were 0, 25, 50, 75, and 100%). The dry weight of the CNF film was first balanced, and then the film was placed in the test solution. After a given interval, the sample was removed from the liquid and wiped briefly and weighed immediately. The liquid up-take of the film was calculated by using Eq. 1.

$$\text{Liquid up - take} \left(\frac{g}{g} \right) = \frac{w_l - w_0}{w_0}, \quad (1)$$

where w_1 is the wet weight of the sample and w_0 is the dry weight of the sample measured before placing it in the liquid. For each time point, separate samples were used. All time points were repeated at least three times.

Surface Plasmon Resonance (SPR) measurements with cellulose nanofibril thin films

Interactions between NMMO and CNF in both pure methanol and water were investigated in real time with a multi-parametric Surface Plasmon Resonance instrument MP-SPR Navi210A (Oy BioNavis Ltd, Finland). The measurements were carried out with the gold-coated SPR sensors carrying spin-coated CNF thin films. The SPR method is based on the phenomenon called surface plasmon resonance (Schasfoort et al. 2008). The SPR phenomenon is highly sensitive to changes in the optical properties of the sensor surface. When molecules from the bulk liquid are adsorbed on the sensor surface, the thickness of the adsorbed layer can be calculated based on the change in the SPR angle (Eq. 2).

$$d = \frac{l_d}{2} \frac{\Delta_{\text{angle}}}{m(n_a - n_0)}, \quad (2)$$

where Δ_{angle} is the change in the MP-SPR angle, l_d is a characteristic evanescent electromagnetic field decay length, estimated as 0.37 of the light wavelength (240 nm), m is a sensitivity factor for the sensor obtained after calibration of the MP-SPR (109.94°/RIU), n_a is the refractive index of the adsorbed substance, and n_0 is the refractive index of the bulk solution. The refractive indices utilized in the estimations were 1.401 for NMMO, 1.325 for pure methanol, and 1.334 for MilliQ-water. The size of an NMMO molecule was estimated to be 0.59 nm by using www.chemicalize.org molecule dimension calculation software. All measurements were repeated at least twice.

The CNF thin films were prepared on gold-coated SPR sensors using spincoating, as described elsewhere (Ahola et al. 2008). Briefly, CNF-gel (0.150 wt% in water) was first ultrasonicated with the 25% amplitude for 10 min by using a 400 W tip sonicator (Brandon 450 Digital Sonifier, Branson Ultrasonics, Danbury,

USA) and subsequently centrifuged (10,400 rpm, 45 min, 25 °C). A part of the clear supernatant was then collected where individual CNFs were located. The gold-coated SPR sensors (Oy BioNavis Ltd., Ylöjärvi, Finland) were first UV/ozonized and then pre-adsorbed with a thin anchoring layer of PEI. Then, the supernatant collected containing individual CNFs was consecutively spin-coated onto the PEI coated sensor at 3000 rpm speed with 90 s spinning time. The spin-coated CNF film was dried at 80 °C for 10 min and stored in a desiccator. Prior to the measurements with MP-SPR, the CNF surface was stabilized in the measurements liquid overnight.

Surface topography of reinforced CNF films with AFM and SEM

The topographical changes on the CNF film after partial dissolution with NMMO were characterized by using Atomic Force Microscopy (AFM) and a Scanning Electron Microscopy (SEM). The imaging with both instruments was carried out using dry specimens without any pre-treatments. The AFM imaging was performed with a Nano-TA scanning probe microscope (Anasys instruments, Santa Barbara, USA). The images were scanned in air with silicon cantilevers operating a tapping mode with the image size of $2.5 \times 2.5 \mu\text{m}^2$. From each sample three separate areas were imaged, and flattening was the only image processing applied. The SEM imaging was carried out with a Merlin FE-SEM (Carl Zeiss NTS GmbH, Germany) without sputter coating. First, the sample was fastened onto an aluminium specimen stub with a double-sided carbon adhesive diss. The imaging was performed using the 1.5 keV electron energy using both secondary electron and InLens detectors. The image pixel resolution was 2048×1536 .

Chemical composition of reinforce CNF films by NMR and FTIR

The changes in the crystallinity of the CNF films after partial dissolution with NMMO were investigated with a ^{13}C cross polarization magic angle spinning (CP MAS) NMR spectrometer (Bruker AVANCE-III 400 MHz, Bruker BioSpin, Germany). For all samples, 20,000 scans were collected using 8 kHz spinning frequency, 2 ms contact time, and 5 s delay between pulses.

The chemical changes in the CNF films with and without partial dissolution were measured with a Thermo Scientific Nicolet iS50 FT-IR spectrometer with an ATR diamond (Thermo Scientific, USA). All spectra were obtained from 32 scans with a resolution of 4 cm^{-1} and transmission mode by using the wavelength range from 400 to 4000 cm^{-1} .

Water diffusion tests

The diffusion of water through the reinforced CNF film was carried out by using a flat sheet membrane Sterlitech CF042 cross/laminar flow test cell (Sterlitech, Kent, USA). The filtration area in the test was 42 cm^2 . The tested film was placed in the filtration cell and subsequently swelled in water overnight. Then the measurement was performed by increasing stepwise the inlet water pressure until the tested film broke down, seen as a drastic rise in the flux through the film. The inlet water pressure and water flux through the film were monitored.

Results

Partial dissolution by NMMO with heat calender assistance

The all-cellulose concept with partial dissolution by NMMO was employed to reinforce CNF films. NMMO monohydrate (referred as NMMO) was first dissolved in pure methanol at a consistency of 25 wt%. Then a pure CNF film was submerged in the prepared NMMO methanol solution. Before the heat activation, the methanol was evaporated from the film structure in the vacuum hood condition. The heat activation was carried out by using a hot calender with a constant calendering roll surface temperature of 130 °C. The heat activation temperature used was found to be a suitable processing condition for “press-welding” with a hot calender. In order to avoid potential side reactions of NMMO lower temperatures, a temperature below 100 °C could be more suited (Johnson 1969; Rosenau et al. 2001). It is important to note that, upon calendering, the film always contains a small proportion of the water from the ambient humidity and the crystalline water of NMMO monohydrate. Moreover, this water is required within the partial dissolution process

(Wachsmann and Diamantoglou 1997; Rosenau et al. 2001). The reinforcing of CNF film with NMMO required a heat activation step, as described elsewhere (Johnson 1969). Without elevated temperature (dried impregnated film was kept in the room temperature), no changes in the properties of a CNF film were observed. We also tested to heat a film carrying NMMO in an oven at 120 °C for 20 min. The achieved reinforcing effect was moderate, supporting the idea of simultaneous heating and mechanical compression. When the CNF film carrying NMMO was passed through the hot calender at a temperature of 130 °C, a drastic change in the transparency of the film was observed (Fig. 1a). This is in accordance with earlier results where all-cellulose composite films were made using NMMO and DMAc/LiCl from paper (Johnson 1969; Nishino and Arimoto 2007). It is important to note here that the heat activation step upon the heat calendaring takes place within a couple of tens of seconds.

The reinforcement with 25% NMMO in pure methanol with heat calendaring increased the film ultimate tensile strength and elongation significantly, from 122 to 174 MPa and 5–11.5%, respectively. The statistics from the mechanical characterization are shown in Table 1. The changes in the film porosity revealed the conceivable reason for the transparency and mechanical properties development. After the NMMO reinforcement, the film porosity declined from 9 to 1%, demonstrating a significant condensation of

the film structure. Conceivably, the NMMO reinforcement increases the fibre–fibre linking via the entanglement (“chemo welding”) of regenerated cellulose chains between neighbouring cellulose nanofibril surfaces. Probably, the film condensation also reduces the number of discontinuation points in the reinforced CNF film, lowering the crack propagation pathways in the film that can also have an effect on the observed rise in the film elongation. The observed increase in elongation was contrary to that reported earlier with CNF films immersed in resins that reduced the CNF film elongation by filling voids on the surface of the CNF films (Henriksson and Berglund 2007; Qing et al. 2013). However, the resin impregnation was shown to elevate the tensile strength similarly as reported, most conceivably due to the hard mechanical nature of dry resins. Polysaccharides have also been utilized to modify CNF films’ mechanical properties, and it is shown that some polysaccharide materials in the fibre–fibre interfaces have improved CNF films’ mechanical properties (Lucenius et al. 2014). The web strength is dominantly affecting on the surfaces, and high density on surfaces should correlate with strength improvement. In this work, it was not possible to measure the density profile through the film. Therefore, the questions around the observed development of mechanical behaviours require more detailed studies.

The effect of the NMMO content in the impregnation solution was investigated. It was observed that the highest mechanical strength and elongation (195 MPa

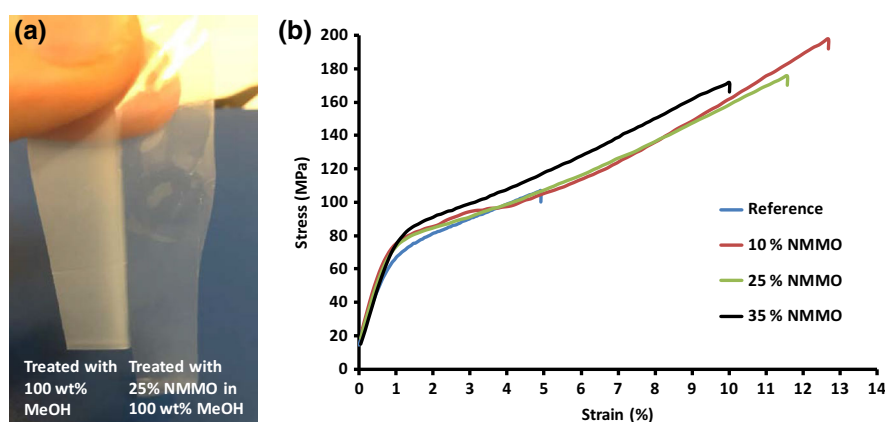


Fig. 1 A photo image of the cellulose nanofibrils (CNF) films with and without partial dissolution with NMMO. **a** The films were impregnated with pure methanol (*left*) or 25% NMMO in pure methanol (*right*) followed by a treatment with a hot calender (130 °C, 1 m/min speed, and approximately 20 kN/m

nip load). Typical tensile stress–strain curves of the CNF films reinforced with and without NMMO and heat activation. **b** The films were impregnated with 10–35% NMMO in pure methanol before the heat activation at 130 °C

Table 1 Mechanical strength of the CNF films with partial dissolution with NMMO from pure methanol and a heat activation

	Reference	10% NMMO	25% NMMO	35% NMMO
Thickness (μm)	24.7 ± 0.5	23.4 ± 0.5	23.9 ± 0.3	23.3 ± 0.3
Density (kg/m^3)	1441 ± 58	1563 ± 43	1590 ± 40	1563 ± 43
Density based porosity (%)	9 ± 1	2 ± 1	1 ± 1	2 ± 1
Tensile strength (MPa)	122.2 ± 20.8	194.6 ± 17.1	173.6 ± 18.4	166.8 ± 21.1
Stiffness (N/m)	77154.0 ± 3481.6	72950.0 ± 3382.6	72691.0 ± 6951.0	80582.0 ± 4723.1
Young's modulus (MPa)	7377.2 ± 495.1	7581.5 ± 650.3	7226.2 ± 979.8	7489.3 ± 679.2
Strain at break (%)	6.7 ± 2.4	13.8 ± 0.8	10.9 ± 1.8	9.4 ± 1.4

and 12.5%, respectively) were achieved with the NMMO consistency of 10% NMMO (Fig. 1b; Table 1). It is possible that the high NMMO consistency elevates the viscosity of the impregnation solution, lowering its diffusion ability into the CNF film pore structure. The NMMO content of the impregnation solution is not the only factor to control the diffusion of NMMO into the film structure. Water has been known to be an effective swelling agent for cellulosic materials. Therefore, liquid-up take studies were performed in order to investigate the effect of the water of the methanol solution on the liquid up-take of film. The liquid up-take into the film structure was improved significantly when the water content in methanol increased (Figure S2, supporting information). With all water contents tested, the plateau level was reached after 30 min, indicating minimum immersion time within the NMMO impregnation. It is important to note that, when high water content (>50%) is used, the processing of the film was difficult due to the drastic softening of the film. It has been reported that the swelling power of methanol for cellulose is a half of that of water (Mantanis et al. 1995). We also tested performing NMMO reinforcement from water–methanol solutions. The porosities of CNF films were much higher than those seen using pure methanol as a solvent. When 25% of water was added into the methanol solution (25% NMMO content), the film porosity was elevated to $25 \pm 2\%$, and the film mechanical strength was 137.8 ± 10.1 MPa. Probably, the water in methanol loosens the film structure more (inter fibre bonding) than the pure methanol, and as the looser film is solidified quickly upon the hot calendering, a more porous structure is formed. The low porosity CNF film may be interesting in applications where improved

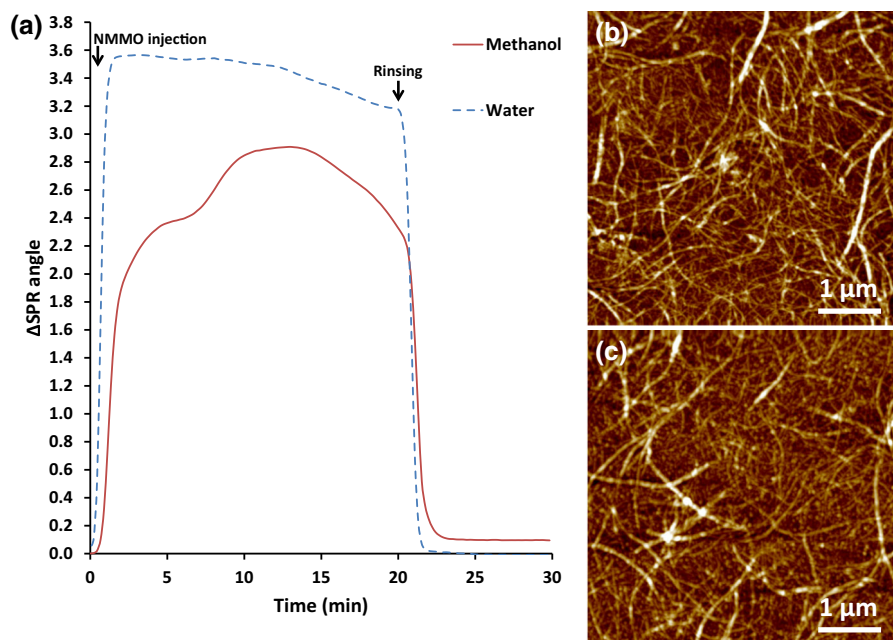
barrier properties are a beneficial material feature, such as with packaging films.

Chemical characterizations

The interactions between NMMO and CNF in two different solvents, pure water and methanol, were investigated by using a surface plasmon resonance (SPR) analysis of nanocellulose thin films. SPR technique is an online method used to investigate molecules interactions with material surfaces. It is capable of measuring the thicknesses of adsorption layers in a nanometre scale. It has been speculated that, upon the dissolution, NMMO interacts with cellulose when the water environment is used (Fink et al. 2001). The secondary aim of the study was to estimate whether NMMO is able to dissolve cellulose at room temperature from diluted solutions. However, the SPR system used in this study does not fully allow the investigations when the liquid is evaporated and the NMMO content increases on the CNF surface. The interaction analyses were carried out at a temperature of 25 °C.

The CNF surfaces were first swelled in the appropriate solvent overnight. Then the solutions containing 25% of NMMO in either pure methanol or pure water were injected onto the CNF surfaces in the measurement chamber (Fig. 2). The injection caused a significant rise in the SPR signals due to the refractivity changes of the bulk media as a result of the dissolved NMMO. After NMMO adsorption, the CNF surfaces were rinsed with appropriated solvents. It can be observed that NMMO adsorbed irreversibly from pure methanol (red curve, the SPR signal did not returned to the baseline level). This difference between the base line and measurement spectra corresponds to a

Fig. 2 SPR sensogram on adsorption of 25% NMMO onto a cellulose nanofibrils (CNF) surface from pure MilliQ water and methanol (a). AFM height images of the CNF surfaces after the adsorption studies with the SPR in pure water (b) and pure methanol (c)



1.2 ± 0.2 nm adsorbed layer (calculated by using Eq. 1). The thickness change correlates with a NMMO bi-layer when the size of a NMMO molecule of 0.59 nm is utilized. In these analysis conditions, no significant changes in the topography of CNF fibrils was observed by AFM (Fig. 2b, c). This is accordance with the information that the dissolution reaction of cellulose requires a low water content and high temperature (Fink et al. 2001). We can, therefore, conclude that, when NMMO is impregnated from methanol, no significant dissolution takes place in the room atmosphere. The study does not, however, show what happens when the solvent is evaporated out. It can also be concluded that methanol is a better solvent than water to utilize in the purification of CNF films after the NMMO treatment.

The changes in the cellulose crystallinity of the reinforced CNF film were investigated with a solid state ^{13}C CP MAS NMR spectrometer (Fig. 3). The reinforcement with 25% NMMO from pure methanol did not change the carbon signal of the bleached cellulose pulp significantly (Larsson et al. 1999). The typical peaks of regenerated cellulose after NMMO dissolution did not appear in the NMR signal (Virtanen and Maunu 2014). This can be used as an indication that only small changes take place in the film during the reinforcement process. The chemical bonding in the reinforced film was investigated

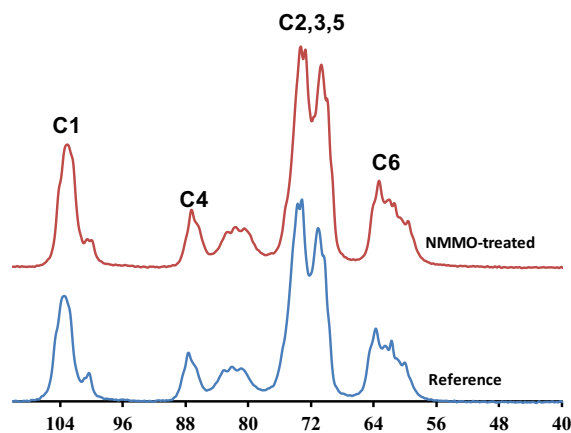


Fig. 3 ^{13}C CP MAS spectrum of pure CNF film before and after partial dissolution with 25% NMMO in 100% MeOH and heat calendering

similarly, also with the FTIR-ATR spectroscopy (Figure S3, supporting information). The results of this investigation were identical, with observations of ^{13}C CP MAS NMR. The stretching and bending vibrations, CH, CH_2 , COH, COC and CO bands, within $1200\text{--}850\text{ cm}^{-1}$ originate from native cellulose molecules (Oh et al. 2005). Change in the morphology of cellulose crystalline structure was not observed, as no peak shifts of the bands at $1022\text{--}1015$ and $895\text{--}990\text{ cm}^{-1}$ corresponding to the CO stretching vibrations at C6 position of the anhydropyranose

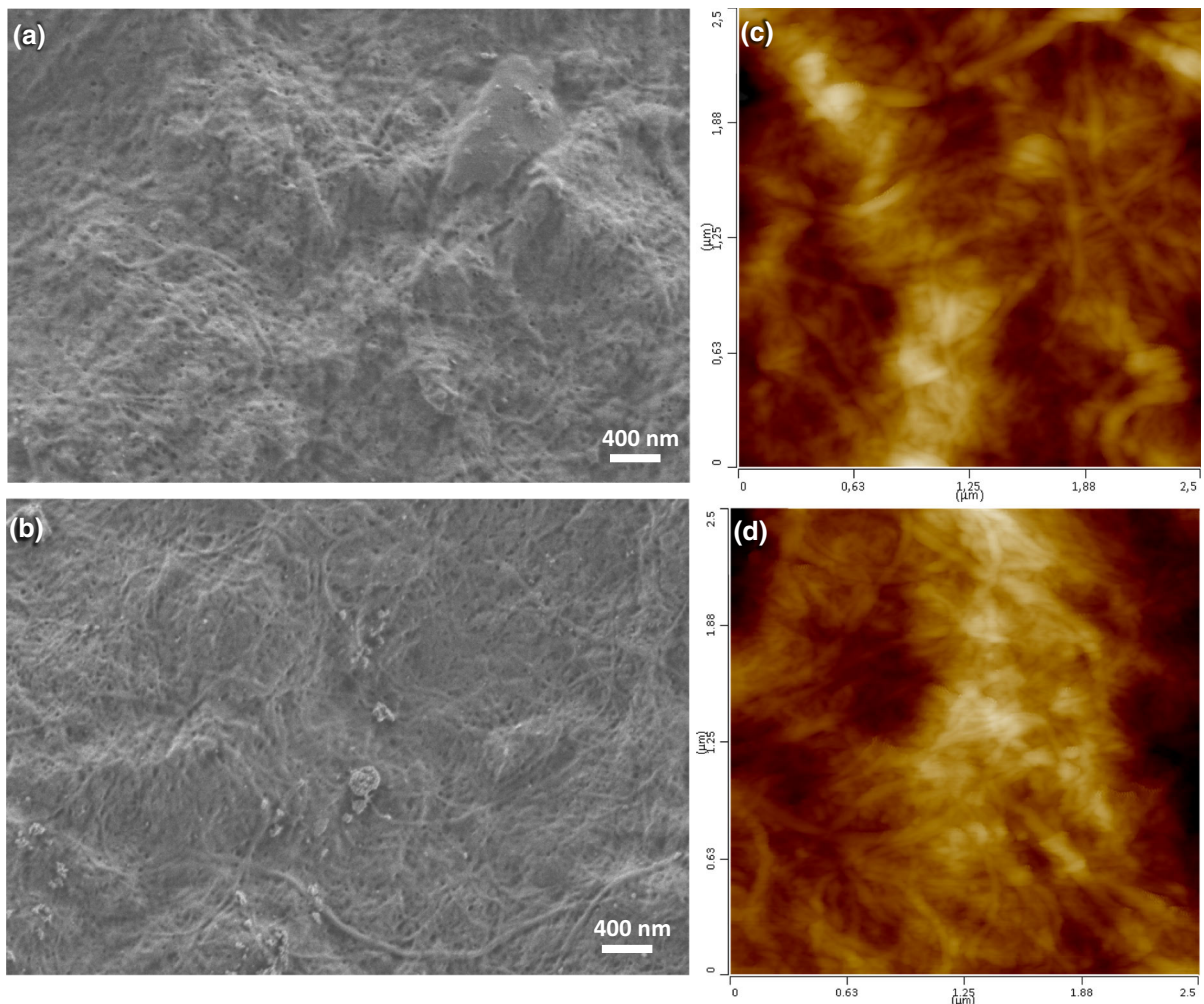


Fig. 4 Surface topography of pure CNF films before (a, c) and after (b, d) partial dissolution with 2% NMMO from pure methanol utilizing the heat activation with hot calendering. a,

b are measured with the Scanning Electron Microscopy and c, d with the Atomic Force Microscopy

occurred. The partial dissolution apparently causes only small changes to the chemical structure of the film, which cannot be observed with the solid-state methods used in this study. We also analysed the water contact angle (WCA) of the CNF film before and after NMMO partial dissolution but no change in WCA was observed (Table T1, supporting information).

The topographical changes on the treated CNF films were investigated with scanning electron microscopy (SEM). The changes on fibril surfaces were characterized from a CNF film treated with 25% NMMO from pure methanol. The treated surface exhibited a fibrillar structure (the side that contacted the metal roll) that was similar to that prior to the

activation (Fig. 4a, b). The treated surface contained some spherical impurities most probably from the calendering process. The same samples were also investigated with the AFM, which has a better resolution for observing nanoscale changes. However, the AFM images revealed fibrillar bundles with thicknesses over 30 nm, which were not significantly degraded during the treatment. It is possible that melted NMMO on the fibril surface causes only local changes on the surface of fibrils, which are not observable in topographical images.

Based on the data from chemical analyses and imaging, we can conclude that the partial dissolution with NMMO by using the (dry) heating technique is a

gentle method. The results give an indication that NMMO molecules are not capable of fully penetrating through the fibrils, probably due to the short heat activation time (only tens of seconds) and a lack of mobile water around NMMO molecules that may contribute to the transportation of NMMO. Because the melting point of NMMO monohydrate is 74 °C, the given NMMO in the film structure will melt in the hot calendering conditions (Fink et al. 2001). NMMO monohydrate melt has been shown to be a powerful solvent for paper surfaces (Johnson 1969). Therefore, it is conceivable that NMMO monohydrate on a fibril surface acts like the NMMO melt dissolving a tiny layer of cellulose, which can link neighbouring fibril surfaces under compression when dissolved cellulose regenerates.

Water resistance of reinforced CNF films

The tensile strength testing was employed to investigate the wet strength of reinforced films. The samples were kept in water for 24 h prior to the measurement. In this study, the extension force was only followed since the accurate film thickness analyses are challenging for wet CNF samples. The pure CNF film (calendered) has a poor or negligible wet strength, as seen from the stress–strain curve (Fig. 5). Cellulose nanofibrils are hygroscopic because they carry tiny layers of water-soluble hemicelluloses on their fibril surfaces (Duchesne et al. 2001). Therefore, when a cast material swells, water easily penetrates into the fibril–fibril interfaces, disrupting the materials’

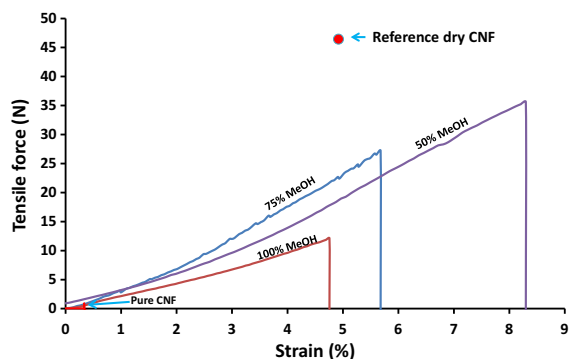
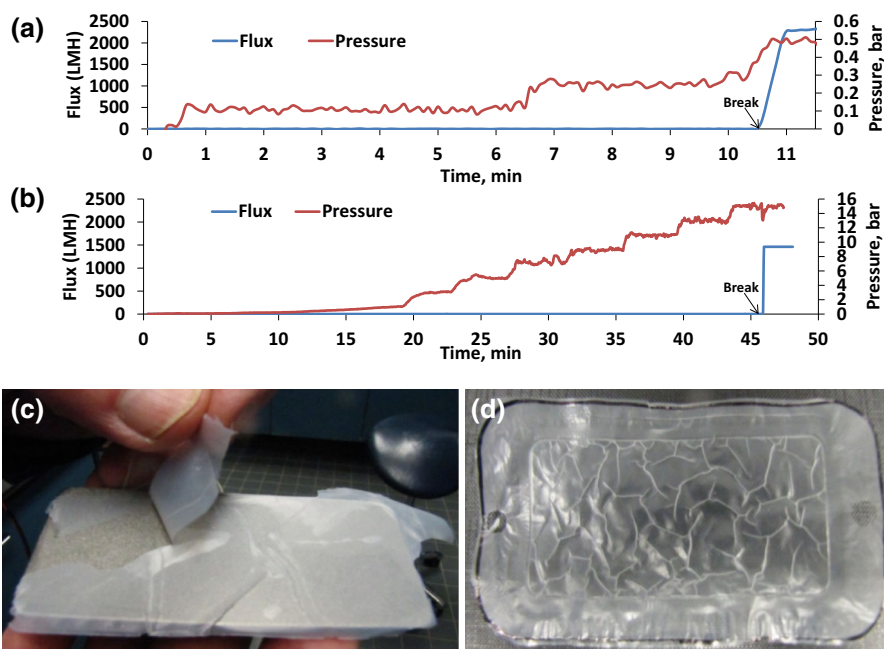


Fig. 5 Typical wet tensile load as a function of the percentage strain of pure CNF and CNF films reinforced with 25% NMMO from 100 and 75% MeOH followed by a heat activation with hot calendering. Before measurement, the films were kept in water for 24 h before measurements were taken

mechanical strength. When the NMMO reinforcement was applied, the wet strength of the CNF film was significantly elevated. The partial surface dissolution with 25% NMMO from pure methanol elevated the ultimate breaking force from 0.25 ± 0.1 to 11.8 ± 1.1 N, that is 25% of the CNF film dry strength. The reinforced CNF film wet strength increased when the water content of the impregnation solution was increased. The highest wet strength (35.6 ± 2.5), which corresponded to the 75% of the dry strength of the pure CNF film, was achieved by using a 50% water content. As we have shown before, CNF films absorb more liquid when the water content of the methanol solution increases (Figure S2, supporting information). Therefore, it is conceivable that the added water in methanol improves the diffusion of NMMO into the film pore structure upon impregnation, and subsequently more fibre–fibre joints can be formed upon the reinforcement, which may explain the higher wet strength. However, in practice, a compromise should be made, because it was shown above that water in the impregnations solution leads to lower dry strength and elevated porosity of film.

The water resistance of reinforced CNF films in elevated water pressures was investigated by using the tangential/crossflow filtration testing. Before the test, the film was swelled in water overnight. The calendered CNF film without an NMMO treatment broke down when the water pressure on the film surface rose above the 0.5 bar (Fig. 5a). Below that, no flux through the film was observed. After a 10-min filtration test, the film was softened to a gel like substance (Fig. 6c). When a CNF film was reinforced with NMMO treatment (25% NMMO in pure methanol), a drastic change in the water pressure resistance was observed. The treated film broke down when the water pressure was raised above 15 bar, but before that no flux through the film was not observed (Fig. 5b). After the filtration test, the film was solid, but visible cracks were observable on the film surface (Fig. 6d). Utilization of CNF in membrane applications has been researched earlier. In those studies, the water resistance for the CNF films was achieved with CNF chemical modification and by adding water resistance chemicals as examples of 2,3-dicarboxylic acid CNF (Visanko et al. 2014) and TEMPO-oxidized CNF with PVA cross-linking (Hakalahti et al. 2016). However, in those studies the membranes were porous, exhibiting a high water flux. To use the

Fig. 6 Diffusion of MilliQ water through pure CNF film without (a) and with reinforcement with 25% NMMO in pure methanol and heat-activated (b) as a function of the water pressure. Before measurement, films were swelled in water overnight. Photo images of pure CNF- (c), and 25% NMMO-treated films (d) after the filtration experiments



NMMO reinforcement in the membrane applications, a porous film structure should be prepared.

All nanofibrillated cellulose composite with regenerated short-cut fibres

The utilization of the NMMO reinforcement with CNF composites with macro scale linear tensile elements was investigated. The poor tear strength is a typical character of pure CNF films that limits their utilization in many applications. The linear elements placed into the composite matrix increase the tearing index of composite remarkably (Ku et al. 2011). Moreover, when cellulosic tensile elements are utilized with a cellulosic matrix a perfect compatibility between matrix components and good biodegradability can be achieved due to the chemical similarities. (Bledzki and Gassan 1999) In this study, a 5% of 1.5 denier lyocell short-cut fibres (length 5 mm) were mixed into pure CNF and then the solution was solvent-cast into a plastic polypropylene film (Fig. 7a). It was observed that lyocell fibres were distributed rather evenly within the CNF matrix, but a clear (machine) directional orientation was visible. From the SEM image, it can be observed that the lyocell fibres were evenly coated by CNF (Fig. 7b). However, the higher magnification image reveals that the CNF layer on an individual

lyocell fibre was not smooth, representing a bulge-like surface structure (Fig. 7). The cross-section of the prepared CNF-short-cut fibre composite was also investigated with the SEM, and clear layering was observed (Figure S4a, supporting information). It can be speculated that the most probable reason for this is the shrinking forces of the suspension caused by the drying that can separate the prepared composite into layers when incompressible large tensile units are present. Cellulose nanofibrils have been used as reinforcement in a large number of composites with varying polymer matrixes without similar problems (Abdul Khalil et al. 2012).

The CNF-short-cut fibre composite film was reinforced with an impregnation with 25% NMMO from pure methanol followed by heat calendering. The treatment solidified the inner part of the composite seen as a removal of the layer-like structure in the SEM image (Figure S4, supporting information). Furthermore, the bulge-like surface structure vanished from the individual short-cut fibres surfaces after treatment (Figure S5, supporting information). The tensile testing was employed in order to study the effect of added short-cut fibres on the mechanical properties of CNF composite. Added short-cut fibres lowered the mechanical strength of the CNF film from 122.2 ± 20.8 to 58.0 ± 6.8 MPa (Fig. 8). Furthermore, the profile of the stress–strain curve differed

Fig. 7 Photo image of the unmodified CNF films with (right) and without (left) 5% of 1.5 denier lyocell short-cut fibres (a). SEM images of a CNF film with 5% of 1.5 denier lyocell short-cut fibres with two different magnifications (b) and (c)

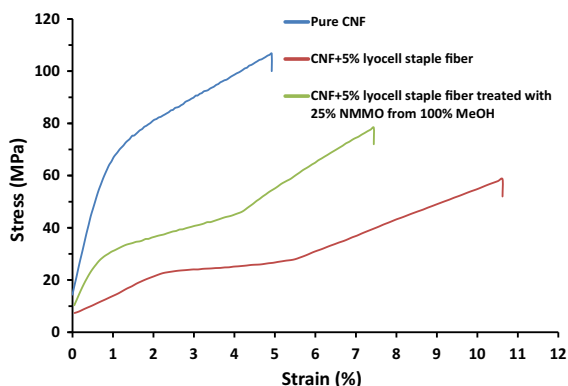
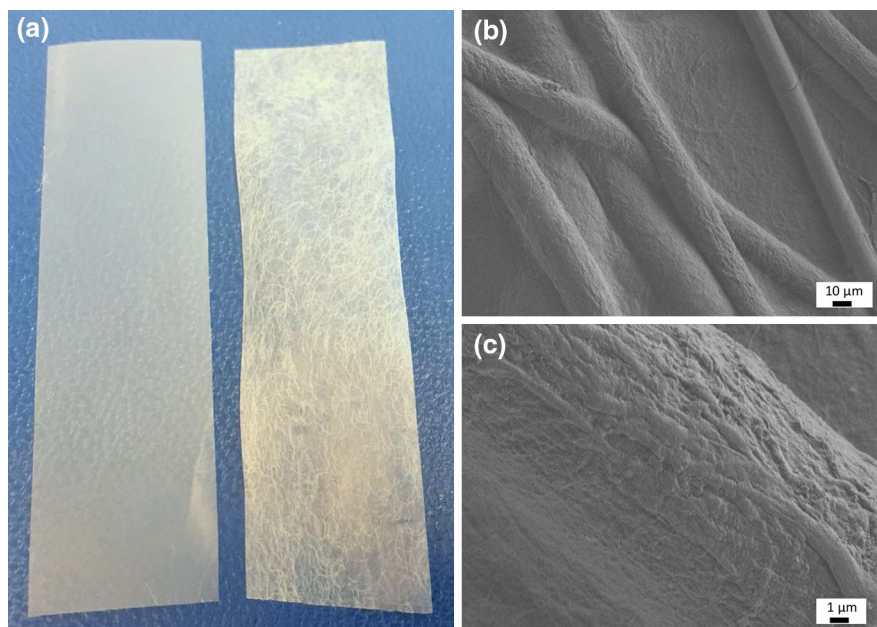


Fig. 8 Typical tensile stress curves as a function of percentage strain of pure CNF, and CNF composites with loaded of 5% lyocell short-cut fibres with and without partial dissolution with NMMO

from that pure CNF, indicating a clear increase in the plastic deformation region, changing the material property from semi-brittle to ductile. However, the short-cut fibres improved the elongation of the CNF film significantly from 6.7 ± 2.4 to $10.5 \pm 2.1\%$. When the CNF-composite was reinforced with partial dissolution with NMMO, the tensile strength of the composite increased 35% simultaneously, decreasing the elongation by 40%. The reason for that is the formation of mechanical linkages between cellulose fibrils and short-cut fibres and condensation of the

structure. With the NMMO treatment, the composite did show a significant water resistance (Figure S6, supporting information). It can be concluded that, after the treatment, the durability of the CNF-composite was remarkably improved, opening new application areas where strong and biodegradable composite materials are needed.

Conclusions

N-methylmorpholine-*N*-oxide (NMMO) can be impregnated into the structure of CNF film by using a liquid as a carrier matrix. After liquid evaporation, NMMO can be melted at moderate temperatures, allowing surface sensitive dissolution that chemically links the reinforced matrix structure. When the simultaneous heating and compression process is used, the film structure achieves its raised mechanical performance. The NMMO impregnation can be controlled with the concentration and water content of NMMO solution. The heat activation by using a hot calender offers a rapid route to heat-activate impregnated CNF films also on an industrial scale. Moreover, the utilization of a hot calender could allow the continuous reinforcing of CNF films. Thus, this fully cellulosic film allows applications where risk of chemical contamination should be avoided. The

developed water-resistant fully cellulosic CNF film has good application potential in applications where non-cellulosic components are not desired and good biodegradability are beneficial factors.

Acknowledgments The work was carried out in the Design Driven Value Chains in the World of Cellulose project (DWOC) funded by Tekes the Finnish Funding Agency for Innovation. The authors also thank the Academy of Finland. The authors appreciate the help given by Unto Tapper (SEM imaging), Tommi Virtanen (NMR analysis), Vuokko Liukkonen (helping with calendering), Hanna Kyllönen (filtration testing), and Salonen Ulla (helping with the tensile testing).

Author contributions The manuscript was written through contributions of all the authors. All authors have given approval to the final version of the manuscript.

References

- Abdul Khalil HPS, Bhat AH, Ireana Yusra AF (2012) Green composites from sustainable cellulose nanofibrils: a review. *Carbohydr Polym* 87:963–979. doi:[10.1016/j.carbpol.2011.08.078](https://doi.org/10.1016/j.carbpol.2011.08.078)
- Ahola S, Salmi J, Johansson L-S et al (2008) Model films from native cellulose nanofibrils. Preparation, swelling, and surface interactions. *Biomacromolecules* 9:1273–1282
- Bledzki AK, Gassan J (1999) Composites reinforced with cellulose based fibres. *Prog Polym Sci* 24:221–274. doi:[10.1016/S0079-6700\(98\)00018-5](https://doi.org/10.1016/S0079-6700(98)00018-5)
- Briassoulis D (2004) An overview on the mechanical behaviour of biodegradable agricultural films. *J Polym Environ* 12:65–81. doi:[10.1023/B:JOOE.0000010052.86786.ef](https://doi.org/10.1023/B:JOOE.0000010052.86786.ef)
- Chanzy H, Nawrot S, Peguy A et al (1982) Phase behavior of the quasiternary system *N*-methylmorpholine-*N*-oxide, water, and cellulose. *J Polym Sci Polym Phys Ed* 20:1909–1924. doi:[10.1002/pol.1982.180201014](https://doi.org/10.1002/pol.1982.180201014)
- Duchesne I, Hult E, Molin U et al (2001) The influence of hemicellulose on fibril aggregation of kraft pulp fibres as revealed by FE-SEM and CP/MAS 13C-NMR. *Cellulose* 8:103–111
- Fink H-P, Weigel P, Purz H, Ganster J (2001) Structure formation of regenerated cellulose materials from NMMO-solutions. *Prog Polym Sci* 26:1473–1524. doi:[10.1016/S0079-6700\(01\)00025-9](https://doi.org/10.1016/S0079-6700(01)00025-9)
- Graenacher C (1934) Cellulose solutions. Patent US1943176
- Hakalahti M, Mautner A, Johansson L-S et al (2016) Direct interfacial modification of nanocellulose films for thermoresponsive membrane templates. *ACS Appl Mater Interfaces* 8:2923–2927. doi:[10.1021/acsami.5b12300](https://doi.org/10.1021/acsami.5b12300)
- Henriksson M, Berglund LA (2007) Structure and properties of cellulose nanocomposite films containing melamine formaldehyde. *J Appl Polym Sci* 106:2817–2824. doi:[10.1002/app.26946](https://doi.org/10.1002/app.26946)
- Henriksson M, Berglund LA, Isaksson P et al (2008) Cellulose nanopaper structures of high toughness. *Biomacromolecules* 9:1579–1585
- Hubbe MA, Rojas OJ (2008) Colloidal stability and aggregation of lignocellulosic materials in aqueous suspension. *BioResources* 3:1419
- Huber T, Müssig J, Curnow O et al (2011) A critical review of all-cellulose composites. *J Mater Sci* 47:1171–1186. doi:[10.1007/s10853-011-5774-3](https://doi.org/10.1007/s10853-011-5774-3)
- Iwamoto S, Isogai A, Iwata T (2011) Structure and mechanical properties of wet-spun fibers made from natural cellulose nanofibers. *Biomacromolecules* 12:831–836. doi:[10.1021/bm101510r](https://doi.org/10.1021/bm101510r)
- Johnson DL (1969) Strengthening swellable fibrous material with an amine oxide. U.S. 3 pp
- Kapanen A, Schettini E, Vox G, Itävaara M (2008) Performance and environmental impact of biodegradable films in agriculture: a field study on protected cultivation. *J Polym Environ* 16:109–122. doi:[10.1007/s10924-008-0091-x](https://doi.org/10.1007/s10924-008-0091-x)
- Klemm D (1998) *Comprehensive cellulose chemistry. Fundamentals and analytical methods, vol 1.* Wiley, Weinheim
- Klemm D, Heublein B, Fink H-P, Bohn A (2005) Cellulose: fascinating biopolymer and sustainable raw material. *Angew Chem Int Ed Engl* 44:3358–3393. doi:[10.1002/anie.200460587](https://doi.org/10.1002/anie.200460587)
- Klemm D, Kramer F, Moritz S et al (2011) Nanocelluloses: a new family of nature-based materials. *Angew Chemie Int Ed* 50:5438–5466
- Ku H, Wang H, Pattarachaiyakoo N, Trada M (2011) A review on the tensile properties of natural fiber reinforced polymer composites. *Compos Part B Eng* 42:856–873. doi:[10.1016/j.compositesb.2011.01.010](https://doi.org/10.1016/j.compositesb.2011.01.010)
- Kurihara T, Isogai A (2014) Properties of poly(acrylamide)/TEMPO-oxidized cellulose nanofibril composite films. *Cellulose* 21:291–299. doi:[10.1007/s10570-013-0124-z](https://doi.org/10.1007/s10570-013-0124-z)
- Larsson PT, Hult E-L, Wickholm K et al (1999) CP/MAS 13C-NMR spectroscopy applied to structure and interaction studies on cellulose I. *Solid State Nucl Magn Reson* 15:31–40. doi:[10.1016/S0926-2040\(99\)00044-2](https://doi.org/10.1016/S0926-2040(99)00044-2)
- Lavoine N, Desloges I, Dufresne A, Bras J (2012) Microfibrillated cellulose—its barrier properties and applications in cellulosic materials: a review. *Carbohydr Polym* 90:735–764. doi:[10.1016/j.carbpol.2012.05.026](https://doi.org/10.1016/j.carbpol.2012.05.026)
- Lucenius J, Parikka K, Österberg M (2014) Nanocomposite films based on cellulose nanofibrils and water-soluble polysaccharides. *React Funct Polym* 85:167–174. doi:[10.1016/j.reactfunctpolym.2014.08.001](https://doi.org/10.1016/j.reactfunctpolym.2014.08.001)
- Mantanis GI, Young RA, Rowell RM (1995) Swelling of compressed cellulose fiber webs in organic liquids. *Cellulose* 2:1–22. doi:[10.1007/BF00812768](https://doi.org/10.1007/BF00812768)
- Moon R, Martini A, Nairn J et al (2011) Cellulose nanomaterials review: structure, properties and nanocomposites. *Chem Soc Rev* 40:3941–3994
- Nishino T, Arimoto N (2007) All-cellulose composite prepared by selective dissolving of fiber surface. *Biomacromolecules* 8:2712–2716. doi:[10.1021/bm0703416](https://doi.org/10.1021/bm0703416)
- Oh SY, Il Yoo D, Shin Y, Seo G (2005) FTIR analysis of cellulose treated with sodium hydroxide and carbon dioxide. *Carbohydr Res* 340:417–428. doi:[10.1016/j.carres.2004.11.027](https://doi.org/10.1016/j.carres.2004.11.027)
- Österberg M, Vartiainen J, Lucenius J et al (2013) A fast method to produce strong NFC films as a platform for barrier and functional materials. *ACS Appl Mater Interfac* 5:4640–4647. doi:[10.1021/am401046x](https://doi.org/10.1021/am401046x)

- Paakko M, Vapaavuori J, Silvennoinen R et al (2008) Long and entangled native cellulose I nanofibers allow flexible aerogels and hierarchically porous templates for functionalities. *Soft Matter* 4:2492–2499. doi:[10.1039/B810371B](https://doi.org/10.1039/B810371B)
- Peresin MS, Vartiainen J, Kunnari V, et al (2012) Large-scale nanofibrillated cellulose film: an overview on its production, properties, and potential applications. In: *Book of abstracts international conference of pulping, papermaking and biotechnology*
- Qing Y, Sabo R, Cai Z, Wu Y (2013) Resin impregnation of cellulose nanofibril films facilitated by water swelling. *Cellulose* 20:303–313. doi:[10.1007/s10570-012-9815-0](https://doi.org/10.1007/s10570-012-9815-0)
- Rosenau T, Potthast A, Sixta H, Kosma P (2001) The chemistry of side reactions and byproduct formation in the system NMMO/cellulose (lyocell process). *Progr Polym Sci* 26:1763–1837
- Schasfoort RBM, Tudos AJ, Gedig ET (2008) *Handbook of surface plasmon resonance*. The Royal Society of Chemistry, Cambridge
- Spoljaric S, Salminen A, Luong N, Seppälä J (2013) Crosslinked nanofibrillated cellulose: poly(acrylic acid) nanocomposite films; enhanced mechanical performance in aqueous environments. *Cellulose* 20:2991–3005. doi:[10.1007/s10570-013-0061-x](https://doi.org/10.1007/s10570-013-0061-x)
- Syverud K, Stenius P (2009) Strength and barrier properties of MFC films. *Cellulose* 16:75–85
- Tammelin T, Hippi U, Salminen A (2013) Method for the preparation of nanofibrillated cellulose (NFC) films on supports. *PCT Int Appl* 13 pp, Chemical Indexing Equivalent to 160:342652
- Toivonen MS, Kurki-Suonio S, Schacher FH et al (2015) Water-resistant, transparent hybrid nanopaper by physical cross-linking with chitosan. *Biomacromolecules* 16:1062–1071. doi:[10.1021/acs.biomac.5b00145](https://doi.org/10.1021/acs.biomac.5b00145)
- Vanderhart DL, Atalla RH (1984) Studies of microstructure in native celluloses using solid-state carbon-13 NMR. *Macromolecules* 17(8):1465–1472
- Virtanen T, Maunu SL (2014) NMR spectroscopic studies on dissolution of softwood pulp with enhanced reactivity. *Cellulose* 21:153–165. doi:[10.1007/s10570-013-0144-8](https://doi.org/10.1007/s10570-013-0144-8)
- Visanko M, Liimatainen H, Sirviö JA et al (2014) Porous thin film barrier layers from 2,3-dicarboxylic acid cellulose nanofibrils for membrane structures. *Carbohydr Polym* 102:584–589. doi:[10.1016/j.carbpol.2013.12.006](https://doi.org/10.1016/j.carbpol.2013.12.006)
- Walther A, Timonen JVI, Díez I et al (2011) Multifunctional high-performance biofibers based on wet-extrusion of renewable native cellulose nanofibrils. *Adv Mater* 23:2924–2928. doi:[10.1002/adma.201100580](https://doi.org/10.1002/adma.201100580)
- Wachsmann U, Diamantoglou M (1997) Potential des NMMO-Verfahrens für Fasern und Membranen. *Das Pap* 51:660–665